

## Report Documentation Page

*Form Approved*  
*OMB No. 0704-0188*

Public reporting burden for the collection of information is estimated to average 1 hour per response, including the time for reviewing instructions, searching existing data sources, gathering and maintaining the data needed, and completing and reviewing the collection of information. Send comments regarding this burden estimate or any other aspect of this collection of information, including suggestions for reducing this burden, to Washington Headquarters Services, Directorate for Information Operations and Reports, 1215 Jefferson Davis Highway, Suite 1204, Arlington VA 22202-4302. Respondents should be aware that notwithstanding any other provision of law, no person shall be subject to a penalty for failing to comply with a collection of information if it does not display a currently valid OMB control number.

1. REPORT DATE <b>MAY 2005</b>	2. REPORT TYPE	3. DATES COVERED <b>00-00-2005 to 00-00-2005</b>			
4. TITLE AND SUBTITLE <b>Efficiency and Threshold Analysis of Resonantly Diode-Laser-Pumped 1.6-<math>\mu</math>m Er:YAG Laser</b>		5a. CONTRACT NUMBER			
		5b. GRANT NUMBER			
		5c. PROGRAM ELEMENT NUMBER			
6. AUTHOR(S)		5d. PROJECT NUMBER			
		5e. TASK NUMBER			
		5f. WORK UNIT NUMBER			
7. PERFORMING ORGANIZATION NAME(S) AND ADDRESS(ES) <b>U.S. Army Research Laboratory, AMSRD-ARL-SE-EO, 2800 Powder Mill Road, Adelphi, MD, 20783</b>		8. PERFORMING ORGANIZATION REPORT NUMBER			
9. SPONSORING/MONITORING AGENCY NAME(S) AND ADDRESS(ES)		10. SPONSOR/MONITOR'S ACRONYM(S)			
		11. SPONSOR/MONITOR'S REPORT NUMBER(S)			
12. DISTRIBUTION/AVAILABILITY STATEMENT <b>Approved for public release; distribution unlimited</b>					
13. SUPPLEMENTARY NOTES <b>CLEO/QELS 2005, 22-27 May, Baltimore, MD</b>					
14. ABSTRACT <b>see report</b>					
15. SUBJECT TERMS					
16. SECURITY CLASSIFICATION OF:			17. LIMITATION OF ABSTRACT <b>Same as Report (SAR)</b>	18. NUMBER OF PAGES <b>3</b>	19a. NAME OF RESPONSIBLE PERSON
a. REPORT <b>unclassified</b>	b. ABSTRACT <b>unclassified</b>	c. THIS PAGE <b>unclassified</b>			

# Efficiency and Threshold Analysis of Resonantly Diode-Laser-Pumped 1.6- $\mu\text{m}$ Er:YAG Laser

Dmitri Garbuzov and Igor Kudryashov

Princeton Lightwave Inc., 2555 US Route 130, Cranbury, New Jersey 08512 dgarbuzov@princetonlightwave.com

Mark Dubinskii

U.S. Army Research Laboratory, AMSRD-ARL-SE-EO, 2800 Powder Mill Road, Adelphi, Maryland 20783 MDubinskii@arl.army.mil

**Abstract:** Resonant diode pumping of the 1.6- $\mu\text{m}$  Er<sup>3+</sup>(1%):YAG laser is reported with the absorbed photon conversion efficiency of 26%. Fluorescence study indicates that upconversion is a dominant mechanism affecting the solid-state laser threshold.

©2005 Optical Society of America

**OCIS codes:** (140.3480) lasers, diode-pumped; (140.3500) lasers, erbium; (140.3580) lasers, solid-state

## 1. Introduction

Yb:YAG solid state lasers (SSL) resonantly pumped by GaAs-diode lasers and operating in quasi-three level scheme demonstrate superior performance among solid state sources of coherent radiation [1]. Resonance pumping approach can be used also for Er:YAG SSL operating in the eye-safe 1.6- $\mu\text{m}$  spectral range. Recently 54% optical-to-optical slope efficiency has been obtained for 1.6- $\mu\text{m}$  Er:YAG SSL resonantly pumped with 1532 nm fiber laser [2].

Reported in this paper are the results of the direct resonant pumping of the 1.6- $\mu\text{m}$  Er<sup>3+</sup>-doped bulk SSL with 1470 nm InGaAsP/InP diode laser. To facilitate the first steps in this new development the high-brightness CW single-mode InP-based diode laser was used for pumping. This diode laser was fabricated from 1470-nm Quantum Well Separated Confinement laser structure and packaged in standard telecom 12-pin butterfly module with polarization maintaining fiber output as described earlier [3].

Absorption and emission peaks in Er<sup>3+</sup>YAG crystals in the spectral range of 1450-1660-nm are due to the transitions between the <sup>4</sup>I<sub>13/2</sub> and <sup>4</sup>I<sub>15/2</sub> Stark-split manifolds forming in Er<sup>3+</sup>:YAG a quasi-three level system (Fig.1). Four upper states out of the eight Stark components of the ground <sup>4</sup>I<sub>15/2</sub> manifold serve as the terminal states for Er<sup>3+</sup> laser transitions with the wavelengths ranging from 1617 to 1660 nm [4].

## 2. DPSSL layout, measurement results and discussion

In the experiments described here, a 4.8-mm-long, 5-mm-dia., Er<sup>3+</sup>(1%):YAG laser rod was single-end pumped in a folded polarization-coupled cavity as shown in Fig. 2. A Polarizing Beamsplitter (PBS) was utilized to separate pumping and lasing radiation paths. A lens L1 and a highly reflective plano-concave mirror M1 (Fig. 2) provide appropriate pumping and laser mode geometric overlap with beam waist radius of about 30  $\mu\text{m}$  in the rod center. Four different flat output couplers (OC) M<sub>2</sub> with transparencies of 0.24%, 3.3%, 9.4% and 13.9% were used to provide variable outcoupling. In addition to the measurement of DPSSL output power the intensities of the infrared fluorescence lines and green upconversion-excited fluorescence have been recorded in these experiments. The infrared fluorescence consists of three components with respective spectral positions of 1646 nm, 1617 nm and 1530 nm. In order to separate these components and measure their respective intensities the overall Er:YAG emission was spectrally decomposed by the 600 groove/mm diffraction grating and measured by an InGaAs photodetector. A Si-photodiode was used for green fluorescence measurement. The intensities of fluorescence spectral components have been recorded with and without output couplers. DPSSL operates in single 1617 nm line with 9.4% and 13.9% OC while at T=3.3% and T=0.23% the spectrum consists of two lines at 1617 nm and 1646 nm.

To record fluorescence intensities and lasing output power as a function of the power absorbed in the YAG rod two photodiodes (PD<sub>i</sub>) and a tilted glass plate (P), shown in Fig. 2, provided reference signals proportional to the incident and unabsorbed pump powers. This component of data acquisition system was calibrated by the signals taken with no rod in the cavity.

The DPSSL output power characteristics measured with different output couplers are shown in Fig. 3. The data were taken at rod temperatures of 20 °C (dashed curves) and 0 °C (solid curves). Drastic increase of the threshold pump power with increasing OC transmission (T) loss prevents SSL from lasing at 20 °C when T=13.9%. The lasing with 13.9% OC has been achieved only with the rod temperature reduction down to 0 °C. The slope of P<sub>out</sub> vs P<sub>abs</sub> is the optical-to-optical efficiency ( $\eta_{\text{opt}}$ ), which, in particular, incorporates a ( $\lambda_{\text{laser}} / \lambda_{\text{pump}}$ ) factor (in our case this

factor is about 0.9). We corrected the values of  $\eta_{\text{opt}}$  by this factor and used the absorbed photon conversion efficiency ( $\eta$ ) instead of  $\eta_{\text{opt}}$  to do the Caird's analysis [5].

Despite of the limited range of the available pump power above the threshold we estimated the absorbed photon conversion efficiency ( $\eta$ ) as  $26\% \pm 3\%$  for the 13.9% OC (Fig. 3). Corresponding values of  $\eta$  for  $T=3.3\%$  and  $9.4\%$  were  $9\%$  and  $20\%$ . These data have been used to perform the Caird's loss and pumping efficiency analysis [5]. By plotting data in the form of

$$\frac{1}{\eta} = \frac{1}{\eta_p} \left[ 1 + \frac{L}{T} \right],$$

where  $T$  is the outcoupling loss,  $\eta$  - photon-to-absorbed-photon efficiency, pumping efficiency of  $\eta_p = 0.37$  and intracavity losses of  $L = 9.2\%$  were inferred (Fig. 4). Using our DPSSL as a probe source the double-path absorption loss in a PBS at  $\lambda=1617$  nm was found to be about  $8\%$  (in a lasing path, see Fig. 2) – most likely because anti-reflective coatings in PBS were designed by manufacturer for  $1550$  nm. It is anticipated that by minimizing intracavity losses the total  $L$ -value can be reduced by an order of magnitude so that  $\eta \rightarrow \eta_p$ .

Obtained low value of  $\eta_p$  is clearly associated with imperfect pump and cavity physical active mode matching in this first experiment and fluorescence intensity data (Fig. 5) confirm this assumption. Indeed,  $1530$  nm and green fluorescence intensities continue to grow at pump powers exceeding the laser threshold. In future experiments we anticipate to considerably improve pump and cavity physical active mode matching to achieve  $\eta_p \cong 1$ .

Data in Fig. 5, collected within 4 orders of magnitude of pump power, indicate the sublinear behavior of the  $1617$  nm and  $1530$  nm fluorescence intensities ( $F$ ) with absorbed power ( $P_p$ ) increase (curves 1 and 2). While at very low pump levels  $F$  is proportional to  $P_p$ , at pumping levels closer to the laser threshold fluorescence intensities  $F$ , are clearly proportional to  $(P_p)^{1/2}$ . This indicates that the two-ion upconversion process is the dominant factor driving the effective lifetime of the excited ions in  ${}^4I_{13/2}$  states. Considering that  $F$  is proportional to the excited  $\text{Er}^{3+}$  ion population in these states and ignoring the depopulation of  ${}^4I_{15/2}$  the system can be treated so that the gain is simply proportional to  $F$ . Fig. 6 indicates that with these assumptions one can explain the fast laser threshold increase with increasing output coupler transparency.  $\Delta F$  values plotted in Fig. 6 were estimated as  $\Delta F = F - F_0$  where  $F_0$  is the  $1617$  nm line intensity at the inversion threshold  $P_i = 25$  mW.  $F$  and  $F_0$  are fluorescence intensity values measured without the OC. The right axis in Fig. 6 indicates the threshold gain values calculated from  $\ln[(1-T)(1-L)]$ , where  $T$  and  $L$  are output and intracavity losses, correspondingly. Solid line 2 in Fig. 6 shows the extrapolation ( $\Delta F$ ) for linear increase of  $F$  with pump power. The differences between positions of experimental points for threshold relative to line 2 are indicative of the threshold increase caused by the upconversion losses. As seen from Fig. 6, more than three-fold increase due to the up-conversion was observed for the  $T=13.9\%$ . This result is in agreement with data obtained from the fluorescence dynamic study in  $\text{Er}^{3+}(1\%):\text{YAG}$  [6].

### 3. Conclusions

We reported resonant diode pumping of the  $1.6\text{-}\mu\text{m}$   $\text{Er}^{3+}$ -doped bulk solid-state laser. Using  $1470$  nm single mode pumping diode laser module, the absorbed photon conversion efficiency of  $26\%$  has been achieved in these first experiments. Analysis of the DPSSL output characteristics indicates that obtained slope efficiency can be doubled through the intracavity loss reduction and pumping efficiency improvement.

Measurements of infrared and green fluorescence intensities versus absorbed pump power clearly indicate that at the excitation levels close to the threshold the upconversion becomes the dominant mechanism limiting the effective lifetime of excited  ${}^4I_{13/2}$  states. It results in super linear increase of the pumping threshold with increasing outcoupling losses. Upconversion impact data are essential for follow-on low-threshold and more efficient resonantly-pumped  $1.6\text{-}\mu\text{m}$   $\text{Er}^{3+}:\text{YAG}$  DPSSL design.

This work was supported by the HEL-JTO/AF through the BAA Contract No.: FA9451-04-C-0189.

### 4. References

1. W. F. Krupke, - IEEE J. of Sel. Top. Quant. Electron. **6** (6), 1287–1296 (2000).
2. Y. Young, S. Setzler, K. Snell, P. Budni, T. Pollak, E. Chicklis, Optics Letters, **29**, p 1075, (2004).
3. D. Garbuzov, I. Kudryashov, A. Komissarov, M. Maiorov, W. Roff, and J. Connolly in Technical Digest of OFC 2003, (OSA, 2003), pp 10-12.
4. N. Agladze, M. Popova, E. Vinogradov, T. Murina, V. Zhekov, Opt. Commun., **65**, p 351, (1988).
5. J. Caird, S. Payne, P. Staver, A. Ramponi, L. Chase, W. Krupke, IEEE J. Quantum Electronics. **QE-24**, p. 1077, (1988).
6. M. Iskandarov, A. Nikitichev, A. Stepanov, J. Opt. Technol., **68(12)**, p. 885, (2001).

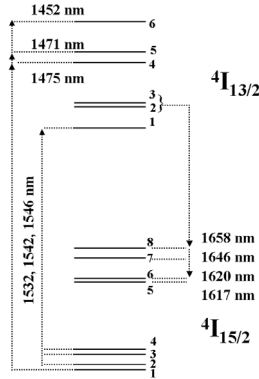


Fig. 1.  $\text{Er}^{3+}$ :YAG absorptive and radiative transitions in the 1.45-1.66  $\mu\text{m}$  spectral range.

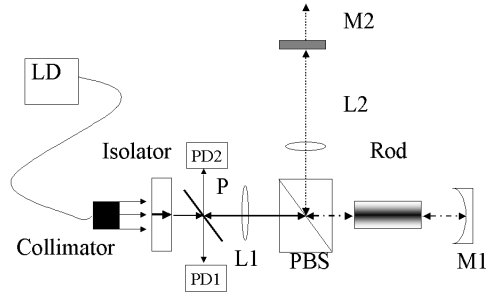


Fig. 2. Resonantly-pumped  $\text{Er}^{3+}$ :YAG DPSSL - optical layout.

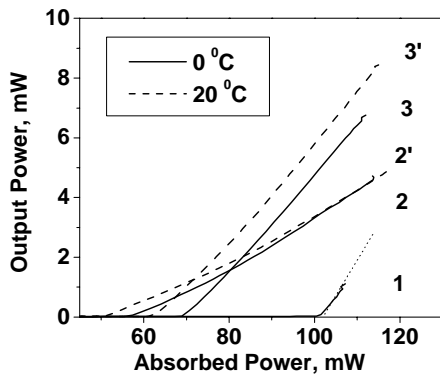


Fig. 3. Output power as a function of absorbed power for 1470-nm pumped  $\text{Er}^{3+}$ :YAG DPSSL with different output couplers: 1 -  $T=3.3\%$ , 2 -  $T=9.4\%$ , 3 -  $T=13.9\%$ . Curves 1, 2 and 3 were measured at rod temperature  $0^\circ\text{C}$  and dashed curves 2', and 3' at  $20^\circ\text{C}$ .

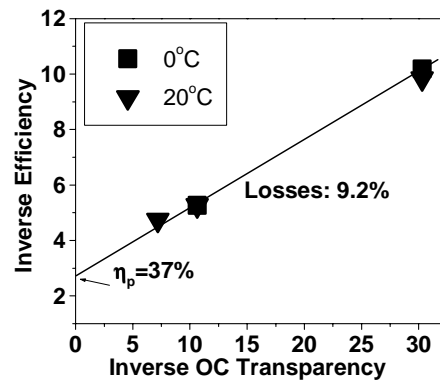


Fig. 4. Inverse absorbed photon conversion efficiency ( $1/\eta$ ) vs. inverse output coupler transmission at  $T=0^\circ\text{C}$  and  $T=20^\circ\text{C}$ .

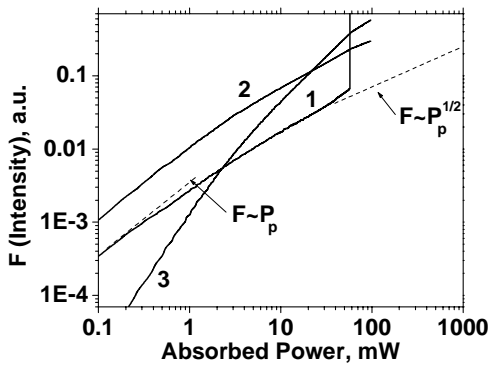


Fig. 5 Fluorescence intensities as a function of the absorbed power measured with 3.4% output coupler. 1 and 2 are for 1617 nm and 1530 nm lines, correspondingly. (3) -green fluorescence. Lasing threshold is seen at 50 mW of absorbed power.

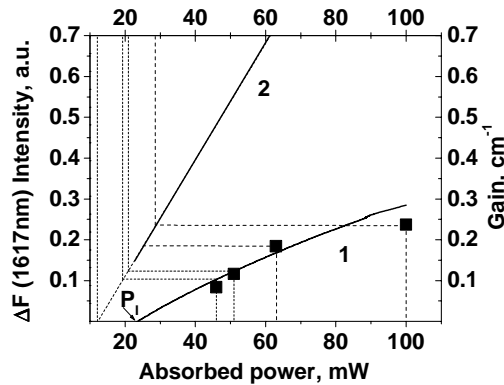


Fig. 6. Curves 1 and 2 (left scale) show the increase of the 1617 nm fluorescence intensities at powers above the inversion threshold. 1- $\Delta F$  from experimental data measured without output coupler, 2- $\Delta F_i$  calculated from the extrapolation of the linear portion of dependence  $F=f(P_p)$  at low excitation level. Solid squares display the threshold gain (right scale) at different output couplers.